https://doi.org/10.2352/ISSN.2470-1173.2017.8.MAAP-279

Adapted Modulation Transfer Function Method for Characterization and Improvement of 3D printed surfaces

Marine Page; Océ Print Logic Technologies, Centre de Recherche et de Restauration des Musées de France, LNE-CNAM; Paris, France.
Gaël Obein; LNE-CNAM; Saint-Denis, France.
Maria Valezzka Ortiz Segovia; Océ Print Logic Technologies; Créteil, France.
Clotilde Boust; Centre de Recherche et de Restauration des Musées de France; Paris, France.
Annick Razet; LNE-CNAM; Saint-Denis, France.

Abstract

2.5D printing is a technology which creates surface relief by superimposing successive layers of inks. The question of the characterization of heights obtained with this technique brings us to consider new metrics and mathematical ways to represent the influence of diverse printing parameters on the obtained relief, possibly used to compensate the defaults of the system.

Our method takes over the classical Modulation Transfer Function (MTF) approach and adapts it to a vertical modulation instead of considering the (x, y) plane, introducing then a Height Modulation Transfer Function (HMTF). Characterization charts are composed of lines patterns printed at different heights, frequencies and droplet levels. Prints are scanned with a chromatic confocal sensor and resulting topographies are analyzed to extract the HMTF. By analogy with traditional MTF methods, results – consisting of the measurement of the deviation between the digital input and the analog output – allow to evaluate the quality of our printer and to compensate it by setting up a retro-action loop.

The method, here presented in the case of the 2.5D printing prototype, can be extended to regular 3D printing techniques.

1. Introduction

2.5D printing is an innovative printing technique based on the successive drop-off of ink layers, shaping a relief in the third Z dimension. The 2.5D prototype printer is capable of creating finely colored and glossy surfaces, at scales going from the ten of microns to several centimeters. This places 2.5D in an interesting position compared to traditional 3D techniques, which are for the moment quite limited in terms of geometry, as only plain facets are printable with an acceptable quality [1].

Museums, exhibition centers, scientific laboratories such as restoration departments seek for non-invasive ways to acquire, copy and reproduce some of their artefacts. Archiving, artefacts conservation, comparisons before and after restoration, educational goals are so many applications we can imagine, targeting as much public and professionals. 3D techniques already answer to some of those purposes [2, 3], especially in the case of large objects, but 2.5D technology still seems to provide a better quality regarding fine details and extent of the color palette.

Nevertheless, some progress needs to be done, for 2.5D such as for 3D, in order to reproduce a genuine copy of a given material, acting at once on color, relief and gloss. In particular, changing the too glossy aspect of the printed surface to a mat finish is still a challenge [4]. The control of appearance properties of a media and of its printable reproduction is thus a crucial point. In this paper, we focus on the control of relief as the first step towards gloss control.

Figure 1: Two details of a fine colored macrotexture reproduced by 2.5D printing: "The Jewish Bride" of Rembrandt. © Eiger Project.

Printing parameters of the 2.5D prototype are numerous and their influence on the appearance of the printed surface not clearly stated. The droplet size, the halftone algorithm, the type of ink, the ink curing time – amongst others – can vary. To carefully reproduce textures and materials, understanding the influence of those printing parameters on the resulting relief is the first step of the characterization of the machine, and may open the way to the compensation of highlighted defects.

2. A metric for relief printing evaluation

To characterize the printer, we need a mathematical tool which represents its performance and their evolution with frequencies. Indeed, we know that printers, like all systems, act as low-pass filter for frequencies: high spatial frequencies are badly transmitted. We used the analogy with optics in order to build a metric which corresponds to our relief printing configuration and based ourselves on the classic Modulation Transfer Function (MTF) method.

2.1 Vocabulary justification and analogies

In two dimensions, for an image appearing in an (x, y) plane, the describing equation of an imaging system is the following convolution product:

$$g(x,y) = h(x,y) * f(x,y) \quad (1)$$

with f the considered object, g the resulting image and h the impulse response of the optical system. After a Fourier transform,

$$G(\mu,\nu) = H(\mu,\nu) \times F(\mu,\nu) \quad (2)$$

with $F = \mathcal{F}(f)$, $G = \mathcal{F}(g)$ and $H = \mathcal{F}(h)$ the Fourier transforms of f, g and h respectively. (μ, ν) are the spatial frequencies corresponding in Fourier to the (x, y) plane. By definition, the magnitude of H is the MTF function, i.e.:

$$|H(\mu,\nu)| = MTF(\mu,\nu) \tag{3}$$

The MTF describes the performance of an optical system by giving a direct and quantitative feedback on the image quality and on the system capacity to transfer details from object to image [5]. In practice, in optics, the computation of MTF consists on the ratio between the contrast of the image and the contrast of the object, using sinusoidal or rectangular patterns at different frequencies. Conversion from CTF (Contrast Transfer Function) to MTF has to be made in case of the rectangular pattern [5, 6, 7]. At a given spatial frequency ν:

$$MTF(\nu) = \frac{Image\ Contrast\ (\nu)}{Object\ Contrast\ (\nu)} < 1 \tag{4}$$

with

$$Contrast = \frac{Intensity_{max} - Intensity_{min}}{Intensity_{max} + Intensity_{min}} \tag{5}$$

The MTF appears as a ratio between the output and the input of the system. This definition is privileged in the specific case of printing.

2.2 State of the art of MTF in printing

MTF is a classical tool in the 2D printing industry and different computation methods exist, mostly distinguishing sinusoidal, rectangular or slanted edges test patterns [5]. Hasegawa et al [8] computes MTF by scanning printed patterns and applying Coltman formulae [7]. Jang & Allebach [9] propose a method to characterize a printer depending on the ink color. Their MTF is defined in the Fourier space as the ratio between a frequency answer and a color difference ΔE. Bonnier & Lindner [10] add that MTF has to be computed for different bias, colors, frequencies, orientations and modulations. Their MTF is a ratio between absorbance values in output and input, deducted from the CIE XYZ coordinates, for each spatial frequency. Al of the above remain in the (x, y) plane.

In the specific 2.5D printing case, regular MTF models have to be extended to the new vertical dimension. In 2013, a study [11] computed quality metrics for relief evaluation. Most of the remarks concerned color or gloss, but the part on relief and texture was limited to examples of shapes measurements in the macro range [12]. A more recent paper [13] focused on this question and proposed a few methods to characterize relief printing. MTF analysis was a part of their work, considering sinusoidal relief targets and frequencies from 7.2 to 57.6 cycles/inch. Our current work aims to improve the quality of their measurements and to extend the use of the MTF as a characterization and compensation tool of relief printing.

2.3 Relief adapted method

To be complete, the MTF concept adapted to relief printing has to be divided into two distinct parts:

- The classical 2D MTF to evaluate performance of the printer into the (x, y) plane. This is the regular configuration case whose measurement methods were above-mentioned.
- The relief MTF on which we focus in this paper and that we will call Height Modulation Transfer Function (HMTF) to avoid confusion. This function gives information on performance of the printer in the Z axis, defined for a given frequency ν as:

$$HMTF(\nu) = \frac{Output\ Height\ Modulation\ (\nu)}{Input\ Height\ Modulation\ (\nu)} \tag{6}$$

with

$$Output\ Height\ Modulation\ (\nu) = \frac{H_{\max output} - H_{\min output}}{H_{\max output} + H_{\min output}} \tag{7}$$

$$Input\ Height\ Modulation\ (\nu) = \frac{H_{\max input} - H_{\min input}}{H_{\max input} + H_{\min input}} \tag{8}$$

By analogy with optics, measurements of contrast and intensity are replaced in this case by measurements of heights. The goal is still to make printing frequencies vary and to observe the response of the printer. The input signal consists on a rectangular pattern as shown Fig. 2.

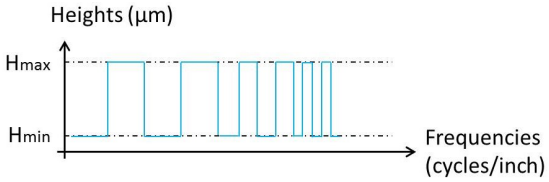

Figure 2: Rectangular input order that is addressed to the printer. Frequencies (in cycles/inch) and chosen heights pairs vary in the protocol.

In the relief case, we have now:

$$g(x,z) = h(x,z) * f(x,z) \tag{9}$$

where f designates the input heights, g the output topography and h stays the unknown function which describes the relief printing system. Heights are defined in the (x, z) plane, as explained Fig. 7. We consider that this function takes into account the whole printing workflow and, by hypothesis, that we can also link its Fourier magnitude to the new HMTF. This equation will allow putting in place a compensation process, as shown in Section 6, assuming the system is linear.

3. Materials and method

The described approach supposes the access to a reliable device for heights measurements. They were performed on a micro-topographic device, the confocal microscope with chromatic coding Stil™ CHR 150N. A halogen lamp sends a white light to a chromatic lens, which breaks down its wavelengths. As shown in Fig. 3, each wavelength strikes at a different height, determined by calibration. A spectrometer analyses the returned reflected wavelength, separated from other reflections by confocal principle, and gives the exact height of the reached point. Thus the information in height is obtained without any shifting along the Z axis. By moving the platform in (x, y), a map of the studied surface is created.

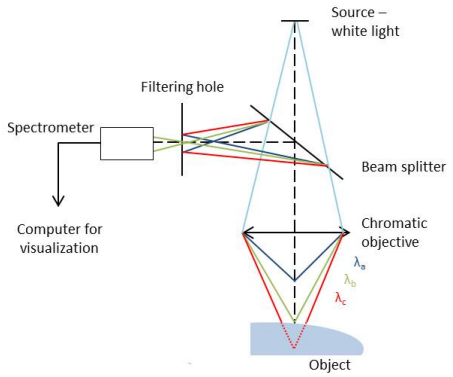

Figure 3: Micro-topographical principle. The white light is decomposed by the chromatic objective. The object reflects a wavelength which comes back to the spectrometer and gives its absolute height.

This system presents a very high lateral resolution and a high signal to noise ratio, which are traditional advantages of the confocal microscopy. Moreover, the information in the vertical axis is reached very easily, without moving the sensor. Resolution in height is around 10 nanometers and 156 nm is the smallest step in (x, y) [14].
The used sensor works at the micro-scale (0-300 µm; numerical aperture 0.43). None of the prints will exceed 200 µm in height for them to stay within the accessible range. Before each measurement session, a roughness calibrated pattern is scanned. Measured values were all the time consistent with expected values. Repeatability of the device is estimated to 0.4 µm, which is low according to the considered [10; 200] µm range of measurements. Thus, for our present study, the device is considered to be robust and accurate.

Data acquisition is performed in accordance with measurement parameters presented Tab. 1. Analyzes of profiles were mostly performed on the Mountains Map © software (Digital Surf™ Company). Fig. 4 presents the measures we considered on acquired profiles.

Measurement range of the sensor	**0 – 300 µm**
Measurement frequency	300 Hz
Scanned lengths in the preliminary tests	25 mm
Scanned lengths in the HMTF protocol	3, 5 or 10 mm
Measurement step in x or y	1 µm

Table 1: Data acquisition parameters of the micro-topographic Stil™ station for all considered printed samples (preliminary tests and HMTF protocol).

Each sample was printed independently 2 or 3 times; measurements of several profiles per print are done with the Stil™ device and heights and lengths measures are computed for several pairs of lines per profile to assure statistical repeatability. All results are then averaged.

All others presented measurements and analyses were performed on Excel™ 2010 and Matlab™ 2016.

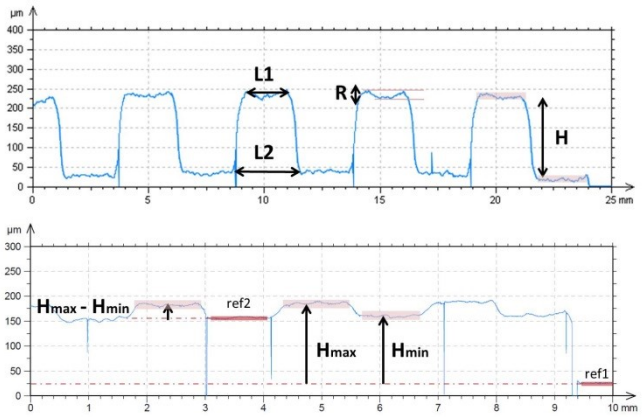

Figure 4: Heights and lenghts measures, at a given frequency, of printed square waves used for the preliminary (top) and HMTF (bottom) studies. L1 designates the length of the upper part of the square wave, L2 the length of the bottom part of the square, R the ringing present on the upper segment and H the height (difference between the mean of the bottom part and the mean of the upper part). "Ref" designates the reference lines, computed with respect to the least square method. Hmax and Hmin are computed as the difference between the mean of heights in their respective segment and the reference line [15]. All values are measured for different bands on a same profile and averaged on at least 3 different profiles.

4. Test protocol

4.1 Preliminary tests

Printing parameters are numerous: droplet size, halftone algorithm, type of ink, ink curing time can for example vary. To focus the HMTF study to relevant parameters only, we looked at the response of the prototype when changing three different parameters: the color of the ink, the UV exposure time and the printing direction. Preliminary tests consist on printing bars of a height of 200µm. Tab. 2 recapitulates the input values. Selected printing parameters are such as their measured heights and lengths are the closest to expected values.

	H	**L1**	**L2**	**R**
Expected values	200 µm	2.5 mm	2.5 mm	0 µm

Table 2: Expected values for the parameters of interest measured on the printed samples during preliminary tests. See Fig. 4 the definition of the parameters H, L1, L2 and R.

Color of the ink:

Only primary colors (cyan, yellow, magenta, black and white) are selected in order to avoid halftone issues. The goal of this study is to determine the best ink, knowing that inks may not have the same fluid flow properties, and also that the micro-topographic device may not scan each colored surface with the same accuracy. Colored bands are printed and analyzed. Analyzing heights and lengths results on Fig. 5, it appeared that cyan ink fits the best.

UV curing time:

Inks dry under UV exposition. The power of UV lamps doesn't change but the exposition time is adjustable to low, median or high exposure times. Cyan bands are printed under the three different UV curing times and analyzed. As a result, on Fig. 6, the minimum exposure time is the better choice for relief creation.

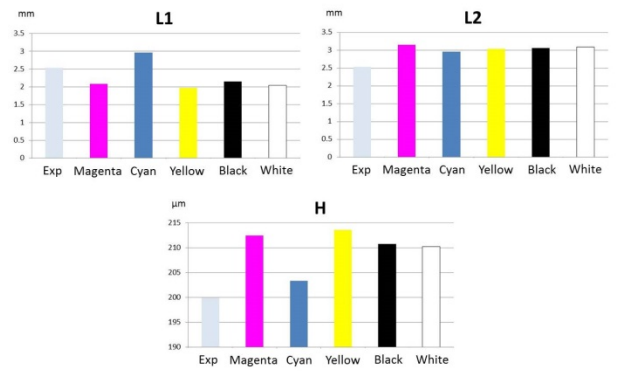

Figure 5: Compared results in heights and lengths for 5 pure inks: magenta, cyan, yellow, black and white. Cyan ink approaches better the expected (exp.) height (H), upper (L1) and bottom (L2) lengths of the profiles and thus is the best ink choice.

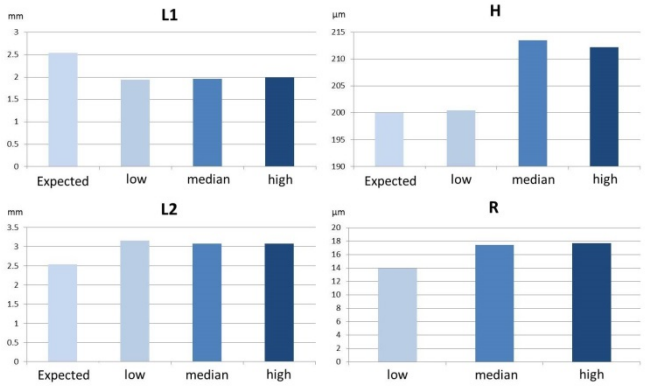

Figure 6: UV study. Histograms represent the results of printed tests at respectively low, median and high UV exposure times. Lengths results (L1 and L2) are quite similar, but the height H, clearly lower for the low time, and the lower ringing allow concluding that the low curing time is the better choice.

Printing direction:

The orientation of patterns during printing, illustrated Fig. 7, affect the resulting print quality, especially when printing periodical patterns.

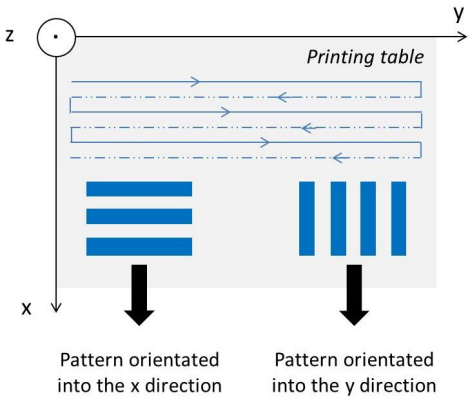

Figure 7: Printing axes. The plane (x, y) represents the printing table and z is the additive relief direction. Blue pointers indicate the way of the printer when active.

Cyan bands are printed orientated in the x and then in the y directions for analysis. By comparing results on heights, lengths and ringing, it appears that the x direction provides a better print quality. This is a natural result given the configuration of the printer; we just add that the difference between expected and obtained heights for the y case is around 20 µm, which is quite important, such as the ringing (20 µm more than in the x case).

Conclusion:

This preliminary study allows us selecting and reducing the list of pertinent printing parameters: for the remained of this paper, we will work in cyan ink, at a 5 millisecond curing time, and print into the x direction.

4.2 HMTF method

The goal is to see both the influence of droplet sizes on printed heights, with respect to different printing frequencies, and the influence of printing frequencies on resulting heights. As mentioned before, the input signal is constituted of rectangular patterns printed at diverse frequencies and heights. Variables are:

- 3 droplet sizes: level 1, level 3 and level 5. They will be referred as lv1, lv3 and lv5 respectively. The correlation between droplet sizes and droplet levels is given Tab. 3.

	Level 1	Level 3	Level 5
Droplet sizes	1.8 µm	5.3 µm	8.8 µm

Table 3: Correlation between droplet level (1, 3 or 5) and physical droplet sizes, in µm.

- 8 spatial printing frequencies: {5, 10, 15, 25, 30, 50, 75, 90} cycles/inch.
- 9 input pairs of micrometric heights, listed on Tab. 4.

	Hmax - Hmin	Hmin	Hmax
_1	11.77	15.68	27.45
_2	28.23	160.00	188.23
_3	32.94	106.67	139.61
_4	44.71	32.94	77.65
_5	54.12	42.35	96.47
_6	58.82	48.63	107.45
_7	78.43	0.00	78.43
_8	89.41	110.59	200.00
_9	127.84	59.61	187.45

Table 4: Input heights instructions (all data are in µm). They are sorted in the growing order for the difference $H_{max} - H_{min}$.

We choose to make vary both H_{max} and H_{min} in order to get more information with a larger panel of considered heights. In total, 648 printed patches were measured three times and 1944 profiles analyzed. Their aspect is shown Fig. 8.

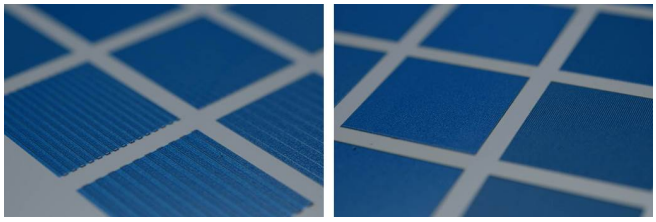

Figure 8: Some printed textures. One single patch corresponds to a square of 1 inch by 1 inch (2.54 cm²).

Height Modulation Transfer Functions are then computed for the entire set of data, and averaged on measurement repetitions and printing sessions. As frequencies are their argument, HMTFs differ according to ordered height pairs.

5. Discussion

5.1 Shape of the curves

Figure 9 shows an example of resulting profiles, for the same frequency (15 cycles/inch) and addressed heights pair, but at different droplet levels. Curves present shapes which are different from the intended rectangular pattern, even at a low frequency. At the first droplet level (lv1) the ringing is pronounced, whereas the roofs of the squares of lv3 and lv5 profiles are sharper.

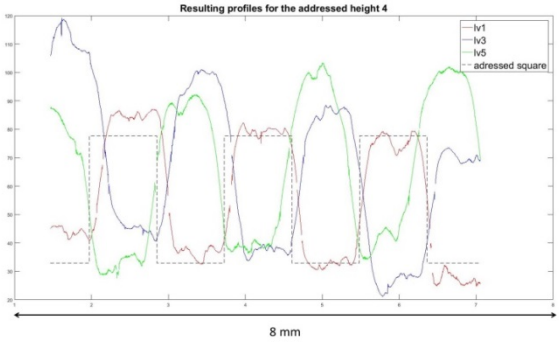

Figure 9: Input rectangular signal (dotted square) and corresponding output signals for three different droplet levels (lv1 in red, lv3 in blue and lv5 in green). Addressed height pair number 4 ($H_{max} - H_{min} = 44.71\ \mu m$). Bars are shifted as measurements days differ. Frequency 15 cycles/inch. At lv1, profiles present an important ringing, as for lv3 and 5, the aspect of the upper length is sharper.

5.2 HMTF

Bode plots of the 9 HMTF were computed; they are showed Fig. 10. Thus we get a representation of the transfer function for each of the considered heights pairs. The model of order n we chose for simulation is following in Eq. 9:

$$HMTF(w) = \frac{H_0}{\sqrt{1+(\frac{w}{w_0})^n}} \tag{10}$$

w is the pulsation, corresponding to the spatial frequency ν by $w = 2\pi\nu$, and H_0 the gain of the system. Fig. 11 presents the evolution of resulting values of parameters from the modeling with the heights pairs and Tab. 5 the obtained ranges of values of H_0, w_0 and n for the three considered droplet sizes.

	lv1	lv3	lv5
H0	$\in [0.28; 0.65]$	$\in [0.29; 0.66]$	$\in [0.31; 0.64]$
w0	$\in [53; 66]$	$\in [45; 62]$	$\in [32; 53]$
n	$\in [4.1; 5.8]$	$\in [3.7; 5.8]$	$\in [2.2; 5.5]$

Table 5: Obtained parameters from the diverse simulations, following Eq. 10.w_0 is in cycles/inch, while H_0 and n are without units. Closest ranges of values are obtained for lv1.

The cut-off frequency w_0 presents many variations, depending most greatly on the droplet level, as shown Tab. 5. The order n of the filter also changes, with droplet levels and heights, being

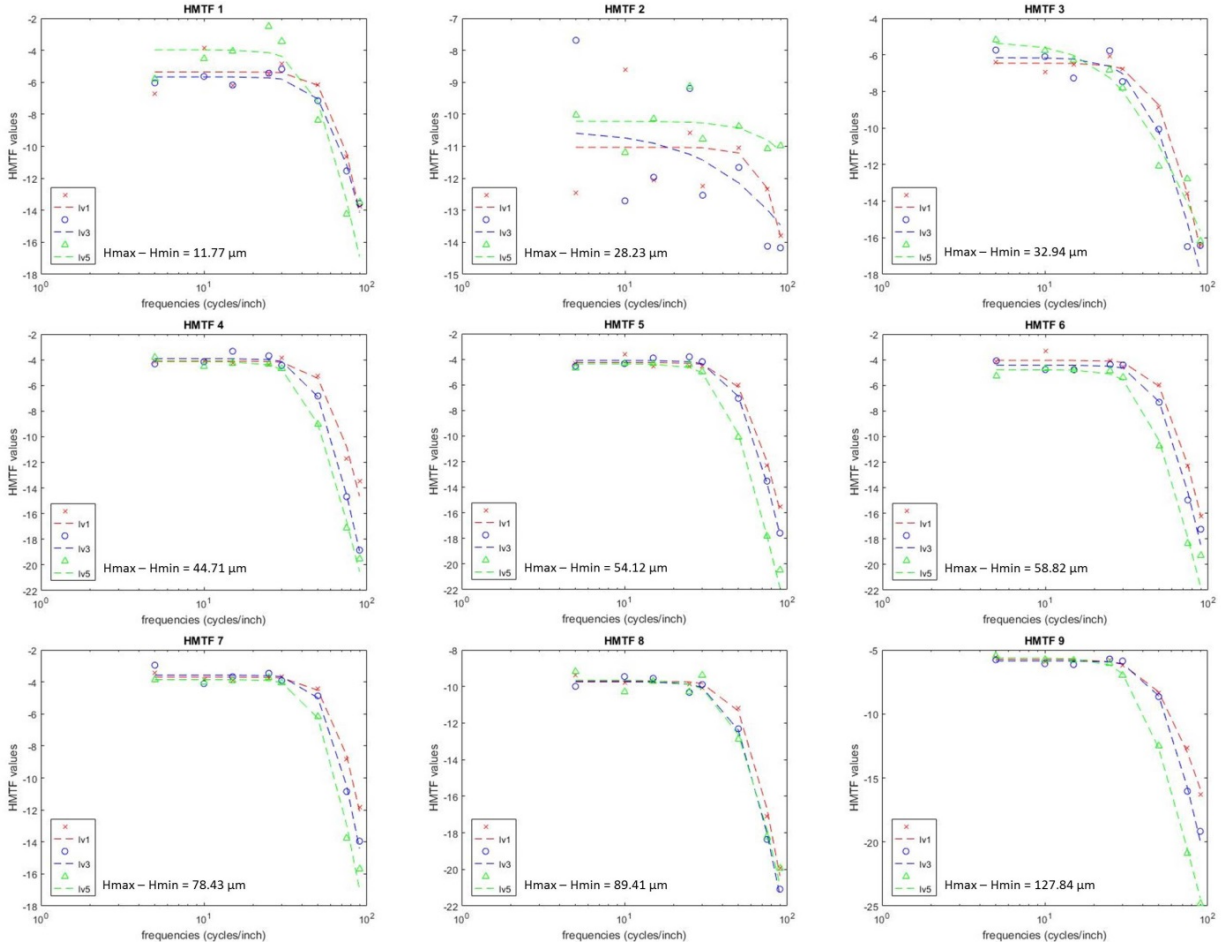

*Figure 10: Bode plots of HMTF of the machine. Frequencies in dB are in abscissas and 20*log(HMTF(w)) in ordinate. Red crosses, blue circles and green triangles are the computed points of the HMTF at the droplet levels 1, 3 and 5 respectively. Dotted red, blue and green lines are the model extracted from the data by minimizing the cost function at the droplet levels 1, 3 and 5 respectively. Each result is different, depending on the considered heights pairs.*

higher for the droplet level 1. Tab. 5 shows that intervals between values, for H_0, w_0 and n, increase with the droplet level. The elaboration of a single model becomes impossible, since variations of w_0 and n are too large to average their values. Nevertheless, the droplet level 1, which presents the smallest variations in the H_0, w_0 and n values, could be resume, for every heights pairs (by averaging them on the computed range) to the function:

$$HMTF(w) = \frac{0.52}{\sqrt{1+(\frac{w}{58.34})^{5.26}}} \quad (11)$$

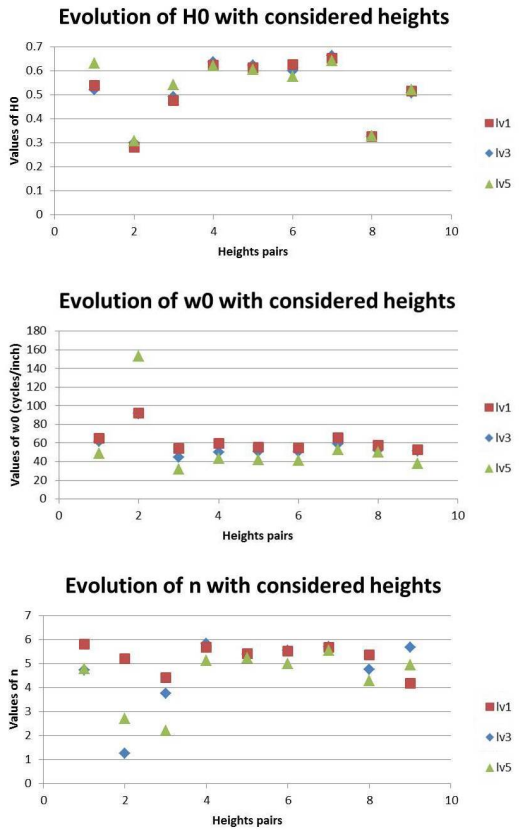

Figure 11: Evolution of H_0, w_0 and n parameters for the three considered droplet levels (1 in red, 3 in blue and 5 in green). In ordinate, values of the parameter (H_0, w_0 or n respectively, from top to bottom) and in abscissa, evolution of heights pairs. Digits refer to Table 4: heights pairs are sorted in the increasing order for the difference $H_{max} - H_{min}$. Values from the case _2, which is very confused, have sometimes been erased in order to let the graphs visible.

Figure 12 shows results in a different manner, based on computed values from measurements (without the dB scale). It appears that the selected droplet size has importance only for high frequencies. Indeed, HMTF behavior for the three considered droplet levels is similar from 5 to 50 cycles/inch, along a large plateau in the short frequencies. After, decline is more or less fast, depending on the droplet level. The computation of cut-off frequencies shows that those values are higher for fine droplets than for large ones (see Fig. 11 and Tab. 5), but nevertheless, concluding that large droplets have to be totally excluded should be too fast. Actually, even if the general trend tends to recommend finer droplets, some surfaces show better performance for large ones, especially in the case where small intervals $H_{max} - H_{min}$ are ordered. This is seen for HMTF_1, HMTF_2 and HMTF_3, on curves from Fig. 10 and surfaces of Fig. 12. Moreover, the fact that performance is quite similar in the [0; 50 cycles/inch] range indicates that for surfaces presenting short spatial frequencies, the use of large droplet can be made as much as fine ones, which would be much faster.

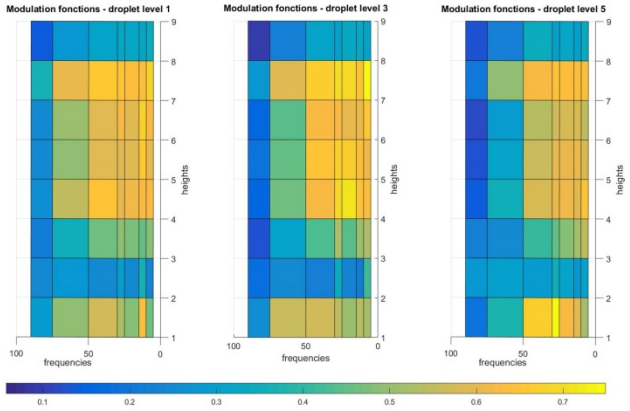

Figure 12: HMTF functions for the 3 droplet levels (1, 3, 5, from left to right). On abscissa, frequencies in cycles/inch are varying. In ordinate, height pairs are changing. The colored scale is similar for the three plots and corresponds to HMTF values.

5.3 Histograms

Figure 13, which is only a representative example extracted from a large set of data, gives us some additional information. Maximum and minimum heights are much higher than expected, but the distance $H_{max} - H_{min}$ in output is close to the expected value, for low frequencies at least.

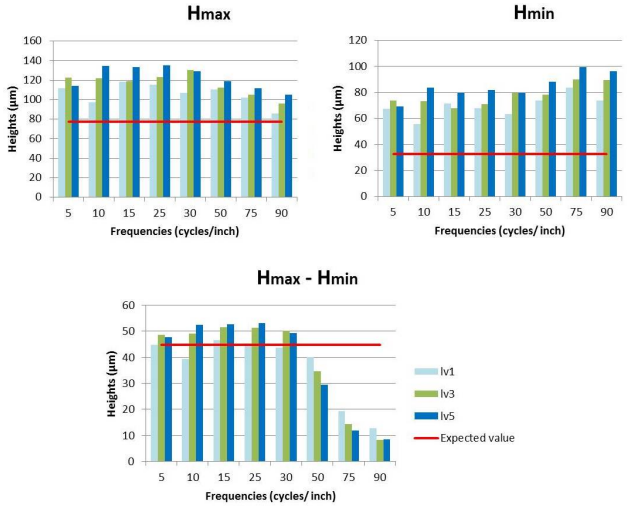

Figure 13: An example of obtained histograms. Addressed height pair number 4 ($H_{max} - H_{min}$ = 44.71 µm). Values have been averaged on the entire data set.

Figure 13 shows that if simple heights are almost never reached, their gap stays quite constant until the frequency 50 cycles/inch where it sharply falls. This behavior is the same for all height couples after averaging. This clearly confirms what we already observed on the HMTF curves, but in practice, it shows the existence of two different problems: first, the necessity to improve

the printing capacity in the high frequencies, and second, the fact that even if HMTF seems to be satisfactory in the short frequencies, the expected heights are not reached.

6. Compensation

6.1 Deconvolution process

Given the HMTF, a deconvolution process can be put in place in order to correct errors of the system. Indeed, as we can write (assessing the linearity of the system):

$$g(x,z) = h(x,z) * f(x,z) \tag{12}$$

by a Fourier transform we have

$$G(\mu,\omega) = H(\mu,\omega) \times F(\mu,\omega) \tag{13}$$

Thus, given that we know H (whose magnitude is the HMTF, see Eq. 3), we can compute a new input signal in order to compensate errors of the output obtained in Session 4. The compensated input signal is the solution of the following deconvolution problem [16]:

$$\mathcal{F}(compensated\ input) = HMTF \times \mathcal{F}(input) \tag{14}$$

whose solution can be written as:

$$\mathcal{F}(compensated\ input) = {\mathcal{F}(input)}/{HMTF} \tag{15}$$

i.e.

$$compensated\ input = \mathcal{F}^{-1}\left({\mathcal{F}(input)}/{HMTF}\right) \tag{16}$$

To reduce the noise, improvement can be made by implementing a Wiener filter [16], written as:

$$compensated\ input = \mathcal{F}^{-1}\left(\frac{\mathcal{F}(input)}{HMTF} \times \frac{HMTF \times HMTF^*}{HMTF \times HMTF^* + NSR}\right) \tag{17}$$

where NSR is the signal-to-noise ratio.

We used the previously measured HMTF to implement the Wiener filter. NSR was set to 1 in the first test. The implementation of this filter led to a new printing session. New patches were analyzed in a similar way as before through micro-topographic instrumentation and new HMTF functions were computed to compare the new performance of the machine and assess our method.

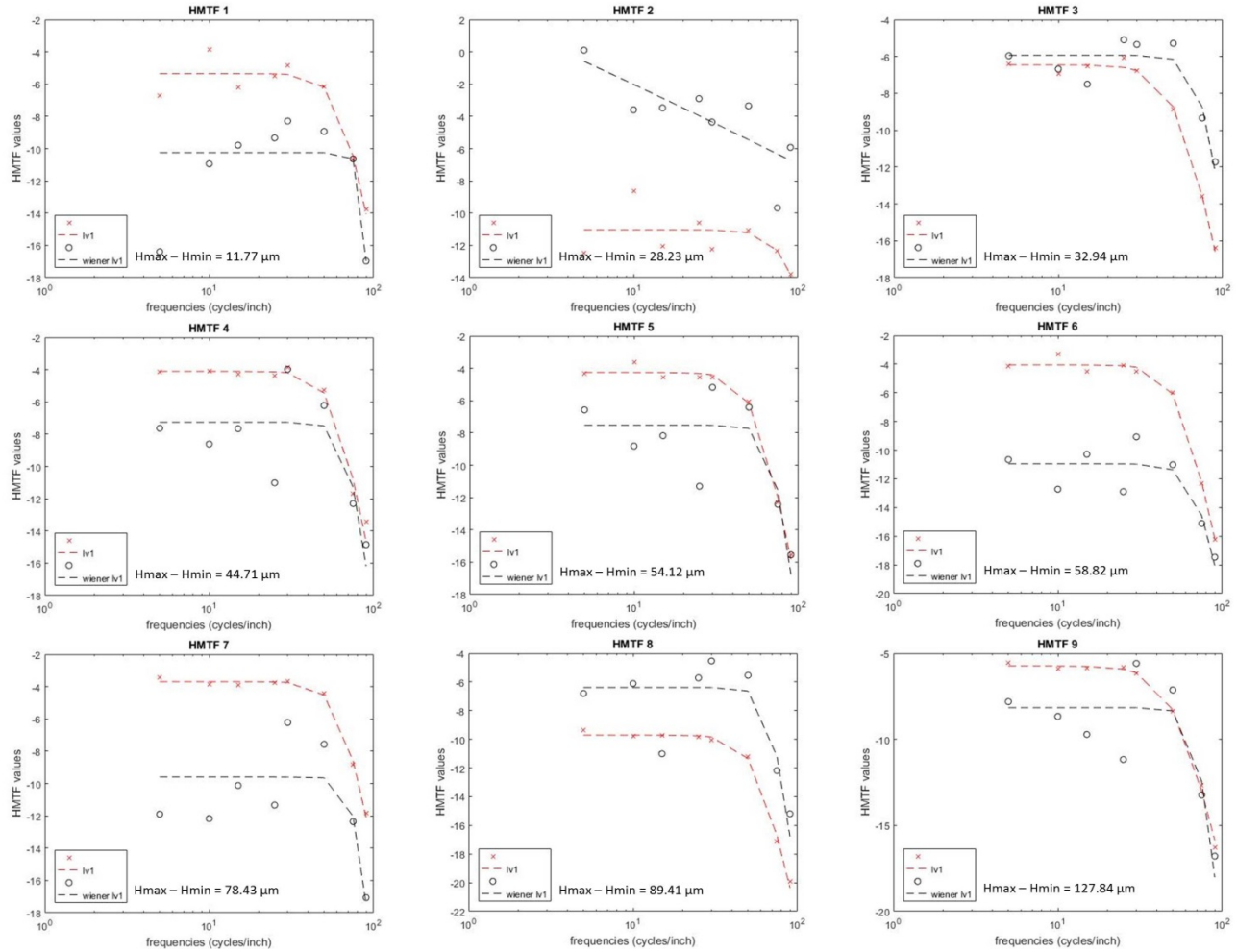

*Figure 14: Compared Bode plots of: regular HMTF (red), for the droplet level 1, with newly computed HMTF (black), after the application of the Wiener filer, for the same droplet level 1. Frequencies in dB are in abscissas and 20*log(HMTF(w)) in ordinate. Red crosses and black circles are the computed points of HMTF. Dotted red and black lines are the model extracted from the data by minimizing the cost function. Only the droplet level 1 is analyzed.*

6.2 Results

Figure 14 presents the results of the compensated printed patches. Black curves are the HMTF which have been corrected through Wiener filtering, and red curves are non-corrected HMTF of Section 5. Two things can be noticed. First, in every case, cut-off frequencies are improved by the applied Wiener filter. Second, some HMTF values are also increased (HMTF_3 and HMTF_8). We can conclude that the use of the Wiener filter was beneficial.

Figure 15 compares the HMTF, for the droplet level 1, previously obtained, with the new Wiener HMTF. We see again that the new HMTF improves performance for certain heights pairs. Fig. 16 shows histograms obtained by applying the Wiener filter. Measured values H_{max} and H_{min} are closer to their expected values, unlike $H_{max} - H_{min}$.

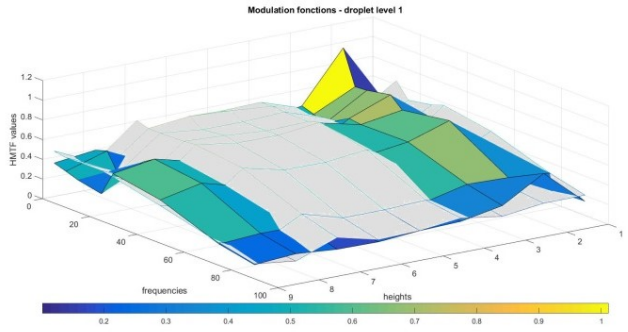

Figure 15: Comparison of regular HMTF, for the droplet level 1 (meshed grey surface), with the new HMTF, computed after the application of the Wiener Filter (colored surface), for the same droplet level 1.Results obtained with the compensation method are better than previously for short and large heights difference. In the middle zone, previous HMTF give better performance.

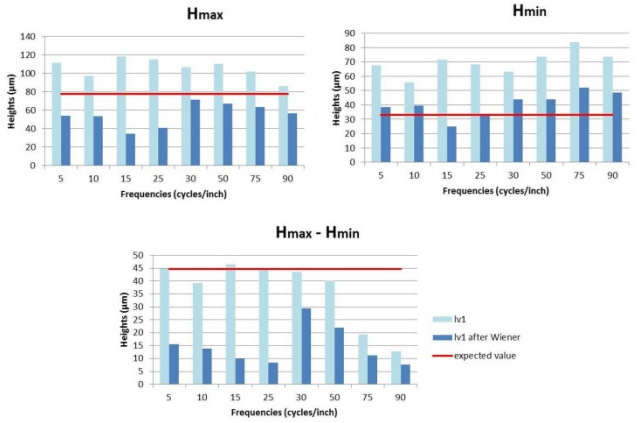

Figure 16: An example of obtained histograms. Addressed height pair number 4 ($H_{max} - H_{min}$ = 44.71 µm). Values have been averaged on the entire data set. Levels 3 and 5 were not printed. Here, heights max and min are close to the expected value (in red), on the contrary to their difference.

6.3 Discussion

Thus, our Wiener compensation was satisfactory on some heights pairs, but not for the whole considered set. An adaptative method, selecting heights, is the next improvement to implement into the printing workflow in order to compensate selectively – only when needed. Moreover, the modeling of the HMTF for the droplet level 1 that we made (see Section 4.2, Eq. 10) will now allow us to directly correct our input signal. Let's add that this part is based on the assumption of the linearity of the printer, assumption we can make because we fixed all parameters (color, orientation), but which is otherwise false [16]. Finely, we add that the estimation of the noise for the computation of the SNR in the Wiener filtering should be strictly made. The stronger the noise is, the low effective is the filter. Other deconvolution techniques could also be tested.

7. Conclusion

In this paper, we selected specific printing conditions: cyan ink, pattern orientated in the x direction, curing time of 5 milliseconds, and we looked at the response in frequencies of the machine, depending on the droplet size and the height order. The HMTF model, together with the high quality measurements we achieve with the micro-topographic device, gives us information on the performance of the 2.5D prototype.

Thus, performance is the same for the three droplet levels until cut-off frequencies of 50 cycles/inch. After, the finer droplet size makes the better results. But it appears also that the machine shows difficulties to produce low heights differences. Nevertheless, our measurements conduct to the establishment of a numerical function which describes the behavior of the printer at the droplet level 1. The assay of compensation through Wiener filtering also succeeds in the improvement of performance for some of the considered heights pairs.

7.1 Limits

A few points have to be mentioned. First, results of this study have to be cautiously extended as we reduced greatly the number of parameters. This was a necessity to avoid too large amounts of data, but it means that this work is valid only for cyan ink, and the specified x orientation of patterns. The others inks, and specially mixed ones in the halftone process, may produce others results. As for the y orientation, it will be characterized in the immediate aftermath of this study.

We also chose to vary both H_{max} and H_{min}, but the offset H_{min} seems to interfere and maybe performance without this offset would be better. Yet, we can also think that with the offset, the protocol is closer from real textures and gives more information in heights.

This method poses many difficulties due to the large amount of parameters, print sessions, and measurement time. It would be necessary to simplify it in order to make this process a regular step of the relief printing workflow.

7.2 Perspectives

This works aims to deal with the question of relief characterization in depth, in order to build an extensive method, usable in 2.5D as for 3D, to represent and compensate printing performance in the z direction. In practice, the goal could be achieved when the protocol could be reduced in terms of parameters and measurements.

This study highlighted that at the micro-scale, the texture space achievable with the prototype relief printer was limited, a problem that future compensation enhancements should solve. But it appeared also that the gloss aspect, for all considered frequencies (from 5 to 90 cycles/inch) is the same for a human observer. Gloss measurements are currently in process to quantify this issue. If we succeed in controlling the printed relief, the next step will be to control the gloss aspect, and especially to create matter textures. By extending the field of printing possibilities, we answer to the wants of cultural heritage art pieces reproduction.

Acknowledgments

The authors greatly thank Christophe Leynadier, Océ PLT, France, for his help and good advice and Ricardo Sapaico, Océ PLT, France, for his thoughtful comments.

References

[1] P. Walters, D. Huson, C. Parraman and M. Stanić, "3D Printing in Colour: Technical Evaluation and Creative Applications", in Impact 6: International Printmaking Conference, Bristol, United Kingdom, 2009.

[2] G. Palidis, A. Koutsoudis, F. Arnaoutoglou, V. Tsioukas and C. Chamzas, "Methods for 3D digitization of Cultural Heritage", in Journal of Cultural Heritage, vol. 8, pp. 93-98, 2007.

[3] C. Schwartz, R. Klein, "Acquisition and Presentation of Virtual Surrogates for Cultural Heritage Artefacts", in EVA: Electronic Visualization and the Arts, pp. 50-57, Berlin, Germany, 2012.

[4] T. Baar, "Optimisation of print quality with multi-channel printing", PhD, Océ Print Logic Technologies, Telecom ParisTech, 2015.

[5] X. Zhang, T. Kashti, D. Kella, T. Frank, D. Shaked, R. Ulichney, M. Fischer and J. Allebach, "Measuring the Modulation Transfer Function of Image Capture Devices: What Do the Numbers Really Mean?", in Proc. SPIE: Image Quality and System Performance IX, Burlingame, California, United States, 2012.

[6] R.L. Lucke, "Deriving the Coltman correction for transforming the bar transfer function to the optical transfer function or the contrast transfer function to the modulation transfer function", Applied Optics, vol. 37, no. 31, pp. 7248-7252, 1998.

[7] J.W. Coltman, "The Specification of Imaging Properties by response to a sine wave input", Journal of Optical Society of America, vol. 44, no. 6, pp. 468-471, 1954.

[8] J. Hasegawa, T.-Y. Hwang, H.-C. Kim, D.-W. Kim and M.-H. Choi, "Measurement-based objective metric for printer resolution", in Proc. SPIE: Image Quality and System Performance IV, San Jose, California, United States, 2007.

[9] W. Jang, J. Allebach, "Characterization of Printer MTF", Journal of Imaging Science and Technology, vol. 50, no. 3, pp. 264-275, 2006.

[10] N. Bonnier, A.J. Lindner, "Measurement and compensation of printer modulation transfer function", Journal of Electronic Imaging, vol.19, iss. 1, 2010.

[11] T. Baar, H. Brettel, M.V. Ortiz Segovia, "A survey of 3D image quality metrics for relief print evaluation", CVCS: Colour and Visual Computing Symposium, Gjovik, Norway, 2013.

[12] C. Polzin, S. Spath and H. Seitz, "Characterization and evaluation of a PMMA-based 3D printing process", Rapid Prototyping Journal, vol. 19, iss. 1, pp. 37-43, 2013.

[13] X. Liu, L. Chen, M.V. Ortiz Segovia, J. Ferwerda, J. Allebach, "Characterization of relief printing", in Proc. SPIE: Measuring, Modeling and Reproducing Material Appearance, San Francisco, California, United States, 2014.

[14] M. Page, C. Boust, N. Mélard, D. Robcis, G. Obein, "3D Surface Acquisiton : Comparison of two microtopograhic Equipments when measuring materials of cultural heritage", in 4th CIE Expert Symposium on Colour and Visual Appearance, Prague, Czech Republic, 2016.

[15] Mountains Map User Manual, Digital Surf, 2011.

[16] N. Bonnier, A. Lindner, C. Leynadier and F. Schmitt, "Compensation of Printer MTFs", in Proc. SPIE: Color Imaging XIV: Displaying, Processing, Hardcopy, and Applications, San Jose, California, United States, 2009.

Author Biography

Marine Page received her BS in optical sciences from the University of Saint-Etienne (France, 2015) and an engineer degree from the Institut d'Optique Graduate School (France, 2015). She is doing her PhD in optical metrology applied to conservation sciences in association with Océ Print Logic Technologies, the Centre de Recherche et de Restauration des Musées de France and the LNE-CNAM (Paris, France – expected graduation in 2019). Her work focuses on the link between relief and gloss.